Toxicology and Applied Pharmacology 243 (2010) 372–380

Contents lists available at ScienceDirect

Toxicology and Applied Pharmacology

journal homepage: www.elsevier.com/locate/ytaap

Perchlorate transport and inhibition of the sodium iodide symporter measured with the yellow fluorescent protein variant YFP-H148Q/I152L

Stefano Cianchetta, Julie di Bernardo, Giovanni Romeo, Kerry J. Rhoden *

Medical Genetics Unit, Department of Gynecologic, Obstetric and Pediatric Sciences, University of Bologna, Bologna, Italy

ARTICLE INFO

Article history:
Received 10 October 2009
Revised 3 December 2009
Accepted 4 December 2009
Available online 18 December 2009

Keywords:
Perchlorate
Iodide
Ion transport
Thyroid gland
Fluorescence microscopy
Environmental contaminant
Cellular assay

ABSTRACT

Perchlorate is an environmental contaminant that impairs thyroid function by interacting with the sodium iodide symporter (NIS), the transporter responsible for iodide uptake in the thyroid gland. Perchlorate is well known as a competitive inhibitor of iodide transport by NIS, and recent evidence demonstrates that NIS can also transport perchlorate. In this study, we evaluated the yellow fluorescent protein (YFP) variant YFP-H148Q/I152L, as a genetically encodable biosensor of intracellular perchlorate concentration monitored by real-time fluorescence microscopy. Fluorescence of recombinant YFP-H148Q/I152L was suppressed by perchlorate and iodide with similar affinities of 1.2 mM and 1.6 mM, respectively. Perchlorate suppressed YFP-H148Q/I152L fluorescence in FRTL-5 thyroid cells and NIS-expressing COS-7 cells, but had no effect on COS-7 cells lacking NIS. Fluorescence changes in FRTL-5 cells were Na^+-dependent, consistent with the Na^+-dependence of NIS activity. Perchlorate uptake in FRTL-5 cells resulted in 10-fold lower intracellular concentrations than iodide uptake, and was characterized by a higher affinity (K_m 4.6 μM for perchlorate and 34.8 μM for iodide) and lower maximal velocity (V_{max} 6.8 μM/s for perchlorate and 39.5 μM/s for iodide). Perchlorate also prevented iodide-induced changes in YFP-H148Q/I152L fluorescence in FRTL-5 cells, with half-maximal inhibition occurring at 1.1–1.6 μM. In conclusion, YFP-H148Q/I152L detects perchlorate accumulation by thyroid and other NIS-expressing cells, and reveals differences in the kinetics of perchlorate versus iodide transport by NIS.

Introduction

Perchlorate (ClO_4^-) is an inorganic anion that is present in the environment naturally and as an industrial contaminant (ITRC, 2005;). It is used as an oxidizer in solid-fuel rockets and missiles, and in the manufacture of explosives, pyrotechnics, dyes and rubber. Inadequate waste management practices have lead to perchlorate groundwater and surface water contamination, particularly at sites in close proximity to military and aerospace facilities and related industries. The detection of perchlorate in public drinking water systems, food crops, forage and commercial milk has triggered public concern over the potential impact of environmental perchlorate on human health (Kirk et al., 2003, 2005; Jackson et al., 2005; NRC, 2005; Sanchez et al., 2005; US EPA, 2008a and 2008b; Murray et al., 2008; Srinivasan and Viraraghavan, 2009). Perchlorate can impair thyroid function by inhibiting thyroidal iodide uptake, and in the past, had therapeutic applications in the treatment of hyperthyroidism and thyrotoxicosis. Thyroid hormones regulate metabolism and are essential for growth and development, particularly during gestation and early infancy. Insufficient iodide uptake can result in hypothyroidism, and in severe cases, delayed development and mental retardation.

Perchlorate is a potent inhibitor of the sodium iodide symporter (NIS), a membrane transporter located on the basolateral surface of thyroid follicular cells (Dai et al., 1996; Dohan et al., 2003). NIS concentrates iodide in the thyroid gland to more than 30 times plasma levels, using the inwardly directed sodium gradient maintained by the sodium potassium ATPase. NIS cotransports sodium and iodide into thyroid cells, and iodide then diffuses into the follicular lumen where thyroid hormone synthesis occurs. Perchlorate competitively inhibits iodide uptake by NIS, reducing its availability for incorporation into thyroglobulin, the precursor of thyroid hormones.

In addition to inhibiting iodide accumulation, perchlorate is also transported by NIS (Dohan et al., 2007; Tran et al., 2008). Perchlorate is accumulated by the thyroid gland (Yu et al., 2002), and *in vivo* studies in rats suggest that thyroidal perchlorate may act directly or indirectly on thyroid hormone synthesis or secretion (McLanahan et al., 2009). NIS is expressed by other iodide-transporting tissues such as the placenta and lactating mammary gland (reviewed by Dohan et al., 2003), and NIS-mediated transfer of perchlorate by these

Abbreviations: 2′-7′-bis(carboxyethyl)-5(6)-carboxyfluorescein acetoxymethyl ester, (BCECF-AM); GFP, green fluorescent protein; GST, glutathione S-transferase; NIS, Sodium Iodide Symporter; PBS, phosphate-buffered solution; pH_i, intracellular pH; YFP, yellow fluorescent protein.

* Corresponding author. U.O. Genetica Medica, Policlinico S. Orsola-Malpighi, Pad. 11, via Massarenti 9, Bologna 40138, Italy. Fax: +39 051 6364004.
E-mail address: kerry.rhoden@unibo.it (K.J. Rhoden).

0041-008X/$ – see front matter © 2009 Elsevier Inc. All rights reserved.
doi:10.1016/j.taap.2009.12.004

tissues may result in fetal/neonatal exposure to the anion. The important health-related consequences of NIS-mediated perchlorate transport highlight the need to measure the cellular uptake of this ion, and characterize the kinetics of its transport by NIS. This has been limited so far due to the difficulty of measuring perchlorate in living systems. Electrophysiological techniques fail to detect perchlorate-induced currents in NIS-expressing cells (Eskandari et al., 1997; Yoshida et al., 1997; Yoshida et al., 1998), and radiotracer uptake is hampered by the low specific activity of radiolabeled perchlorate ($^{36}ClO_4^-$). Recently, total perchlorate accumulation by thyroid cells was measured by ion chromatography tandem mass spectrometry (Tran et al., 2008), however the kinetics of transport were not addressed.

Previously, we developed a novel cell-based assay to measure iodide transport by NIS using a genetically-encodable fluorescent biosensor (Rhoden et al., 2007; Rhoden et al., 2008). The biosensor, YFP-H148Q/I152L, is a variant of green fluorescent protein (GFP) derived from the jellyfish *Aequoria Victoria*. YFP-H148Q/I152L fluorescence is sensitive to several halides and pseudohalides, with anion binding causing a decrease in fluorescence intensity (Galietta et al., 2001a, 2001b). The aim of this study was to determine whether YFP-H148Q/I152L was also sensitive to perchlorate and could be used as a biosensor to monitor NIS-mediated cellular uptake of perchlorate *in vitro*. The biosensor was tested in thyroid cells expressing endogenous NIS and in nonthyroidal cells expressing NIS after gene transfer. The biosensor was used to compare the kinetics of iodide and perchlorate transport by NIS, and to assess the ability of perchlorate to inhibit iodide transport.

Materials and methods

Production of recombinant YFP-H148Q/I152L. The YFP-H148Q/I152L open reading frame was cloned into the bacterial expression vector pGEX-4T-1 (GE Healthcare) in frame with the glutathione S-transferase (GST) gene. *Escherichia coli* BL21(DE3) bacteria were transformed with the GEX-4T-1-YFP-H148Q/I152L vector and protein production was induced with 0.5 mM isopropyl-β-D-1-thiogalactopyranoside for 5 h. Bacteria were lysed in 50 mM phosphate-buffered saline (pH 7.4) containing 1% NP-40, 5 mM EDTA, 0.4 mg/ml lysozyme and protease inhibitors (Complete Roche inhibitor cocktail). The GST-YFP-H148Q/I152L fusion protein was purified by glutathione agarose affinity chromatography and eluted from the column in a chloride-free buffer consisting of 50 mM sodium phosphate (pH 8.8), 25 mM reduced free glutathione and 200 mM sodium gluconate.

Cell culture and transfection. Fischer rat thyroid FRTL-5 cells were cultured in Coon's Modified F12 Medium supplemented with 5% newborn calf serum, 1 μg/ml insulin, 3.6 ng/ml hydrocortisone, 5 μg/ml apotransferrin, 10 ng/ml Gly-His-Lys acetate, 10 ng/ml somatostatin, 1 mU/ml TSH, 100 U/ml penicillin and 100 μg/ml streptomycin (Ambesi-Impiombato et al., 1980). Cells were passaged with a Ca^{2+}- and Mg^{2+}-free Hank's balanced salt solution containing 20 U/ml collagenase, 0.75 mg/ml trypsin and 2% dialyzed chicken serum. An FRTL-5 cell line with stable expression of YFP-H148Q/I152L has been previously generated and described (Rhoden et al., 2007). COS-7 cells were cultured in Dulbecco's Modified Eagle's Medium supplemented with 10% fetal bovine serum, 100 U/ml penicillin and 100 μg/ml streptomycin. COS-7 cells were cultured on coverslips in 6-well plates, and were transfected with plasmid cDNA to induce transient expression of human NIS (hNIS) and YFP-H148Q/I152L. Cells were transfected with pcDNA3.1 vectors containing the full-length hNIS coding sequence (donated by S. Jhiang, Ohio State University) or the YFP-H148Q/I152L coding sequence (donated by L.J.V. Galietta, Istituto Giannina Gaslini, Genova, Italy). Transfection was carried out with Lipofectamine 2000 according to manufacturer's instructions (Invitrogen Inc.), using 2 μg cDNA and 6 μl Lipofectamine per well for 5 h. Fluorescence experiments were performed 2–3 days after transfection.

YFP-H148Q/I152L fluorescence imaging. Cells were grown on round glass coverslips and mounted in a thermostatically-controlled perfusion chamber for real-time fluorescence imaging. Fluorescence was monitored with a Zeiss Axiovert 200 inverted microscope equipped with a 40× oil immersion objective, an XBO Xenon 75W short arc lamp, Lambda 10C filter changer (Sutter Instrument Company; Crisel Instruments, Rome, Italy), and XF104-2 YFP filter set for excitation at 500 ± 12.5 nm and emission at 545 ± 17.5 nm (Omega Optical; Crisel Instruments, Rome, Italy). Images were acquired for 100 ms every 10s with a Coolsnap HQ CCD camera (Roper Scientific; Crisel Instruments, Rome, Italy). Fluorescence intensity within a selected region of interest containing 50–100 cells was quantified with Metafluor software (Universal Imaging Corporation; Crisel Instruments, Rome, Italy). Background fluorescence, measured in a region of the coverslip without cells, was subtracted from all measurements.

Cells were continuously perfused at 37 °C with phosphate-buffered saline (PBS) consisting of 137 mM NaCl, 2.7 mM KCl, 0.7 mM $CaCl_2$, 1.1 mM $MgCl_2$, 1.5 mM KH_2PO_4, 8.1 mM Na_2HPO_4 and 10 mM glucose (pH 7.4). Changes in cellular fluorescence due to iodide or perchlorate influx were monitored by exposing cells to PBS containing 1–1000 μM NaI or $NaClO_4$ for 5 min. Cl^- free PBS was prepared by replacing all chloride salts with gluconate salts on an equimolar basis. The effects of extracellular Na^+ on perchlorate-induced responses were studied in a HEPES-buffered solution (HBS) composed of 145 mM NaCl, 5 mM KCl, 0.7 mM $CaCl_2$, 1.1 mM $MgCl_2$, 10 mM HEPES and 10 mM glucose (pH 7.4). Low-Na^+ HBS containing 10 mM Na^+ was prepared by replacing NaCl with equimolar choline chloride.

Baseline fluorescence of cells maintained in PBS was fitted by non-linear regression to a third order polynomial equation in order to correct for fluorescence decay due to photobleaching and spontaneous changes in resting fluorescence which may occur over prolonged periods of time. Fluorescence in the presence of iodide or perchlorate was normalized at each time point to the fitted baseline fluorescence. Intracellular iodide and perchlorate concentrations ($[I^-]_i$ and $[ClO_4^-]_i$ respectively) were calculated according to the equation $[X] = K_a(F_{max} - F) / (F - F_{min})$ where F is the normalized fluorescence at each extracellular anion concentration ([X]), F_{max} is fluorescence in the absence of anions (defined as 1), F_{min} is fluorescence in the presence of saturating concentrations of anions, and K_a is the affinity constant of YFP-H148Q/I152L for iodide or perchlorate. F_{min} and K_a were obtained by *in situ* calibration of YFP-H148Q/I152L fluorescence in FRTL-5 cells (see next section). For each anion, the increase in intracellular concentration over time was fitted to a one-phase exponential association equation, and the maximal rate of anion influx ($d[I^-]/dt$ or $d[ClO_4^-]/dt$) was obtained from the derivative of the best fit curve. The relationship between influx rate and extracellular concentration was analysed according to the Michaelis–Menten equation in order to derive K_m and V_{max} values for iodide and perchlorate uptake. Curve-fitting and derivation of fluorescence and kinetic parameters was performed with Prism (Graph Pad Software, San Diego, CA, USA).

In vitro and in situ calibration of YFP-H148Q/I152L. YFP-H148Q/I152L fluorescence was calibrated with respect to its anion sensitivity using purified recombinant protein (*in vitro* calibration) and YFP-H148Q/I152L-expressing FRTL-5 cells permeabilized with ionophores (*in situ* calibration). Fluorescence was monitored with an inverted fluorescence microscope equipped with a YFP filter set as described in a previous section.

In vitro calibration was used to determine the sensitivity of YFP-H148Q/I152L to iodide, perchlorate and chloride. Purified recombinant YFP-H148Q/I152L was diluted 20-fold in 50 mM sodium phosphate buffer (pH 7.4) containing 300 mM Na gluconate. Specific iodide, perchlorate and chloride concentrations were obtained by substituting sodium gluconate with 0.01–300 mM sodium iodide or sodium perchlorate on an equimolar basis. Aliquots (5 μl) of the YFP-

H148Q/I152L-containing solution were deposited on a coverslip, and triplicate images were captured for fluorescence quantification.

In situ calibration was performed as described previously (Rhoden et al., 2008) to determine the perchlorate sensitivity of YFP-H148Q/I152L expressed in FRTL-5 cells. YFP-H148Q/I152L-expressing FRTL-5 cells were grown on coverslips and mounted in a perfusion chamber maintained at 37 °C for real-time fluorescence imaging. Following an initial perfusion in PBS, cells were exposed to a high-K^+ solution (10 mM HEPES pH 7, 130 mM potassium gluconate, 15 mM potassium chloride) containing nigericin (5 μM), valinomycin (5 μM), and tributyltin (10 μM). Specific perchlorate concentrations were achieved by replacing potassium gluconate with equimolar potassium perchlorate. Cells were perfused with increasing concentrations of perchlorate, and steady-state fluorescence at each concentration was normalized to fluorescence in the absence of perchlorate.

Following *in vitro* and *in vivo* calibration, affinity constants (K_a) were determined by non-linear regression using the four-parameter logistic equation $F = F_{min} + (F_{max} - F_{min}) / (1 + 10\exp(\log K_a - \log[X])\, n)$, where F is the fluorescence at each anion concentration ([X]), F_{max} is the maximal fluorescence in the absence of anions, F_{min} is the residual fluorescence in the presence of saturating concentrations of anions, K_a is the anion concentration causing a 50% of maximal decrease in fluorescence, and n is the Hill slope. The K_a for iodide was previously determined to be 3.5 mM (Rhoden et al., 2008).

Intracellular pH measurement. Intracellular pH (pH_i) was monitored by real-time fluorescence microscopy with the pH-sensitive fluorescent indicator 2′-7′-bis(carboxyethyl)-5(6)-carboxyfluorescein (BCECF). Wild-type FRTL-5 cells (lacking YFP-H148Q/I152L) were grown on coverslips and incubated for 45 min in culture medium containing 10 μM of the acetoxymethyl ester of BCECF (BCECF-AM). Cells were rinsed and incubated for a further 20 min with culture medium to allow for the hydrolysis of BCECF-AM. Coverslips were mounted in the imaging chamber, perfused with PBS at 37 °C and fluorescence monitored at excitation and emission wavelengths of 500 ± 12.5 nm and 545 ± 17.5 nm respectively as for YFP-H148Q/I152L. In order to correct for fluorescence decay due to photobleaching and dye leakage, baseline fluorescence was monitored for 5–10 min in PBS, fitted to a one-phase exponential decay function and fluorescence at each time point expressed relative to the fitted baseline. The effect of perchlorate and iodide on pH_i was assessed by exposing cells to PBS containing 1 mM NaI or $NaClO_4$. At the end of each experiment BCECF fluorescence was calibrated by exposing cells to a high K^+ solution (HEPES 10 mM, KCl 130 mM, $CaCl_2$ 0.7 mM) at pH 6.5–8.0 in the presence of 7μM nigericin and 5 μM valinomycin.

Statistical analysis. Data are presented as mean ± SE of n replicate experiments. Statistical differences between groups were determined by Student's t-test or analysis of variance (ANOVA) where appropriate, using GraphPad Prism software (La Jolla, CA).

Results

Anion-sensitivity of YFP-H148Q/I152L fluorescence

The sensitivity of YFP-H148Q/I152L fluorescence to perchlorate was first assessed using purified recombinant protein, and was compared to the protein's sensitivity to iodide and chloride. YFP-H148Q/I152L fluorescence was suppressed by perchlorate and iodide with similar affinities of 1.2 mM (log K_a −2.91+0.04, n=6) and 1.6 mM (log K_a −2.78+0.03, n=6) respectively (Fig. 1A). Both anions caused near complete (>95%) suppression at 100 mM. Chloride suppressed YFP-H148Q/I152L fluorescence with a lower affinity of 39 mM (log K_a −1.41+0.06, n=6). Hill slopes for all three anions were close to 1 (iodide 0.94, perchlorate 0.92, chloride 1.00), confirming binding of each anion at a single site.

In situ calibration was performed in YFP-H148Q/I152L-expressing FRTL-5 cells in order to measure perchlorate sensitivity in an intracellular environment (Fig. 1B and 1C). Cells were exposed to a high K^+ solution containing ion-selective ionophores tributyltin, nigericin and valinomycin in order allow equilibration of intracellular and extracellular anions and pH (Rhoden et al., 2008). Tributyltin is an anion/OH^- exchanger (Wieth and Tosteson, 1979; Wuthier et al., 1984). Nigericin is an H^+/K^+ ionophore which allows equilibration of pH_i with extracellular pH when cells are maintained in a high-K^+ solution to eliminate the transmembrane K^+ concentration gradient (Thomas et al., 1979). The K^+-selective ionophore valinomycin was included to facilitate equilibration of intracellular and extracellular K^+ concentration. *In situ* calibration was performed at pH 7 and in the presence of 15 mM Cl^- to mimic pH_i and chloride concentration in FRTL-5 cells (Rhoden et al., 2008). Under these conditions, YFP-H148Q/I152L fluorescence was suppressed by perchlorate with an affinity of 2.8 mM (log K_a −2.55 ± 0.03, n=4). The sensitivity of YFP-H148Q/I152L to iodide was previously determined by *in situ* calibration to be 3.5 mM (Rhoden et al., 2008).

Effect of perchlorate on YFP-H148Q/I152L fluorescence in FRTL-5 thyroid cells

Exposure of YFP-H148Q/I152L-expressing FRTL-5 cells to extracellular perchlorate induced a rapid decrease in cellular fluorescence commencing within seconds of exposure and reaching a steady-state

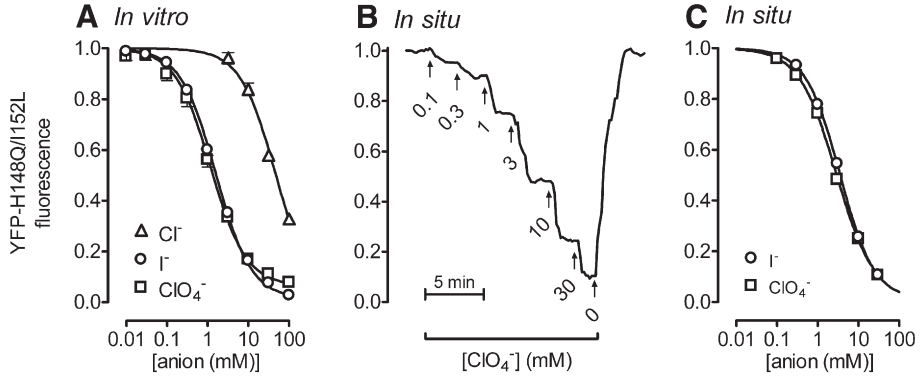

Fig. 1. Anion sensitivity of YFP-H148Q/I152L fluorescence. (A) *In vitro* calibration using purified recombinant YFP-H148Q/I152L in phosphate buffer (pH 7.4) in the presence of iodide (○), perchlorate (□) or chloride (△). Data points represent mean ± SE of 4 measurements. (B) Representative tracing illustrating the *in situ* calibration of YFP-H148Q/I152L in FRTL-5 cells in a high K^+ buffer (pH 7) containing the ionophores nigericin, valinomycin and tributyltin, and increasing concentrations of perchlorate. (C) *In situ* calibration of YFP-H148Q/I152L in FRTL-5 cells for perchlorate (□) and iodide (○). Data points represent mean ± SE of 4 experiments. Iodide data in (C) are reproduced from Rhoden et al., 2008, and are included for comparison.

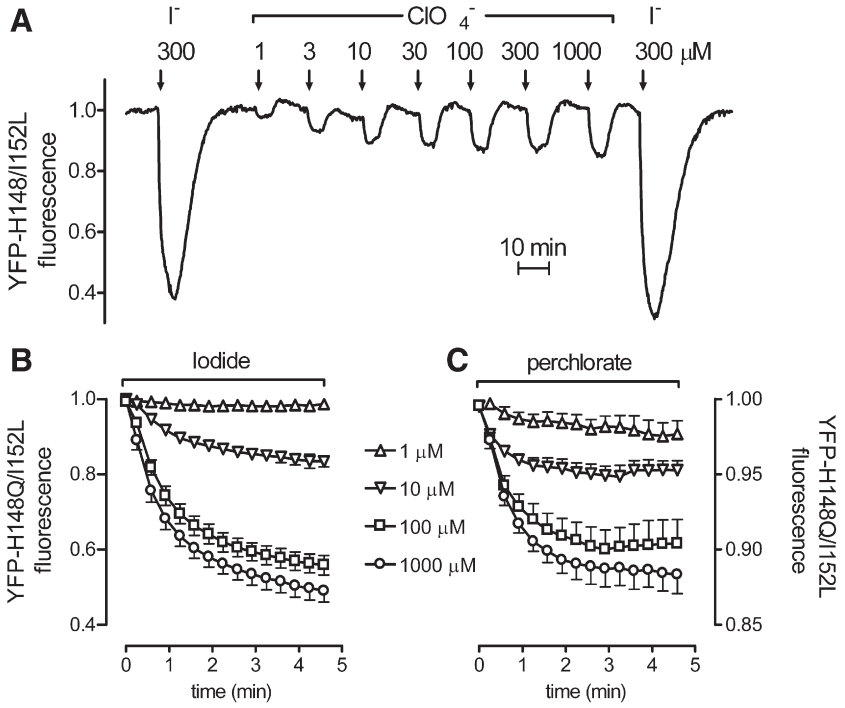

Fig. 2. Effect of perchlorate and iodide on YFP-H148Q/I152L fluorescence in FRTL-5 cells. (A) Representative tracing illustrating iodide- and perchlorate-induced changes in fluorescence, normalized against resting fluorescence. Cells were exposed to iodide or perchlorate for 5 min, followed by rinsing with PBS. Panels (B) and (C) show the time course of fluorescence changes induced by extracellular iodide and perchlorate respectively, at concentrations of 1 μM (△), 10 μM (▽), 100 μM (□) and 1000 μM (○). Data points represent mean ± SE of 6 experiments.

level within 2–3 min (Fig. 2). The magnitude of the fluorescence response was concentration-dependent over the 1–1000 μM range. Iodide also decreases YFP-H148Q/I152L fluorescence in FRTL-5 cells as a result of NIS-mediated uptake and binding to the intracellular fluorochrome (Rhoden et al., 2007). Fluorescence changes induced by extracellular perchlorate, however, were significantly smaller than those induced by iodide, with a maximal decrease in fluorescence after 5 min exposure of 11.7 ± 1.3% for 1 mM perchlorate ($n = 6$) and 51.4 ± 3.0% for 1 mM iodide ($n = 6$) ($p < 0.001$, unpaired t-test). Fluorescence responses to perchlorate were reversible, with complete recovery of resting fluorescence following removal of extracellular perchlorate. Repeated applications of perchlorate produced reproducible responses over time, permitting multiple exposures to perchlorate to be carried out in a single preparation.

Since YFP-H148Q/I152L has not been previously used to detect perchlorate uptake, it was necessary to rule out an indirect effect of perchlorate on intracellular parameters that may affect YFP-H148Q/I152L fluorescence, such as pH_i and Cl^- concentration. The role of pH_i was investigated by examining the effect of perchlorate on pH_i using BCECF. Perchlorate (1 mM) had no effect on BCECF fluorescence in wild-type FRTL5-cells (Fig. 3A). The role of chloride was investigated by measuring the effect of perchlorate on YFP-H148Q/I152L fluorescence in FRTL-5 cells in a medium lacking chloride. Exposure of FRTL-5 cells to Cl^- free PBS caused a 45% increase in resting fluorescence (consistent with the loss of intracellular chloride), but did not affect the suppression of fluorescence by perchlorate (Fig. 3B). These results suggest that perchlorate-induced changes in YFP-H148Q/I152L fluorescence in FRTL-5 cells are not

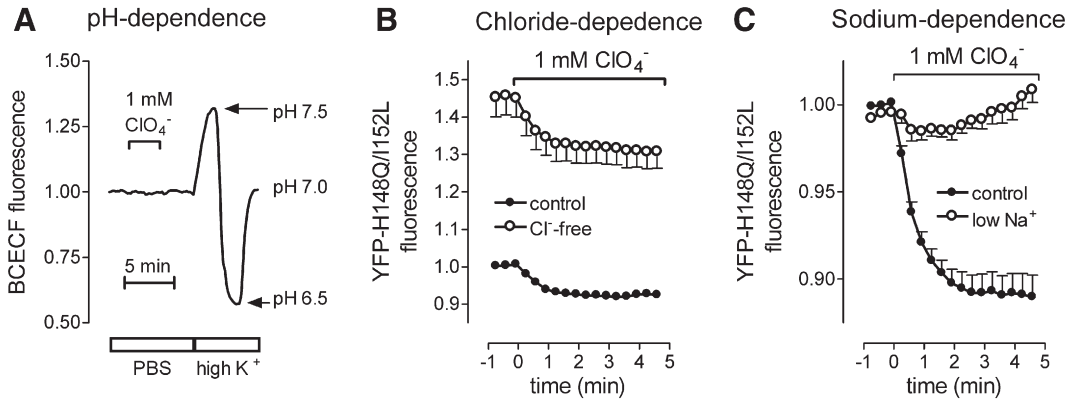

Fig. 3. Role of pH, chloride and sodium. (A) Effect of perchlorate on intracellular pH monitored in FRTL-5 cells with BCECF (representative tracing). Cells were loaded with BCECF for 45 min, and cellular fluorescence was monitored during exposure to 1 mM perchlorate. pH-sensitivity of BCECF fluorescence was confirmed by exposing cells to a high K^+ solution at pH 6.5–7.5 in the presence of nigericin and valinomycin. (B) Effect of extracellular chloride on YFP-H148Q/I152L fluorescence in FRTL-5 cells. Cells were exposed to 1 mM perchlorate in PBS containing 143.3 mM chloride (control) or no chloride (Cl^- free). Data points represent mean ± SE of 8 experiments. (C) Effect of extracellular Na^+ on YFP-H148Q/I152L fluorescence in FRTL-5 cells. Cells were exposed to 1 mM perchlorate in HBSS containing 145 mM Na^+ (control) or 10 mM Na^+ (low Na^+). Data points represent mean ± SE of 7 experiments.

secondary to changes in pH_i or chloride content, but are more likely to reflect transport of perchlorate into cells and a direct interaction with the fluorescent protein.

NIS-mediated anion transport is dependent upon extracellular Na^+ (Eskandari et al., 1997). The Na^+-dependence of perchlorate-induced fluorescence responses was examined by lowering extracellular Na^+ from 145 to 10 mM through isotonic replacement of NaCl with choline chloride. This manipulation prevented the perchlorate-induced suppression of YFP-H148Q/I152L fluorescence (Fig. 3C), confirming that fluorescence responses are Na^+-dependent and compatible with NIS-mediated transport of perchlorate into cells. Previously, iodide-induced suppression of YFP-H148Q/I152L fluorescence in FRTL-5 cells was also demonstrated to be dependent upon extracellular Na^+ (Rhoden et al., 2007).

Quantitation of perchlorate uptake in FRTL-5 thyroid cells

Perchlorate and iodide uptake into FRTL-5 cells was quantified from fluorescence changes, using the measured affinities of YFP-H148Q/I152L derived by *in situ* calibration (perchlorate K_a 2.8 mM, iodide K_a 3.5 mM). The limit of detection of intracellular ions was determined by measuring the smallest detectable change in cellular fluorescence and extrapolating the corresponding iodide or perchlorate concentration from the calibration curve to each ion. A significant change in cellular fluorescence was defined as a change of at least 3 times the standard deviation (3×SD) of resting fluorescence, sustained for the 5-min duration of iodide or perchlorate exposure and reversible upon rinsing with PBS. Using these criteria, the minimum detectable change in cellular fluorescence was ±2.1% (equivalent to 3×SD of the resting fluorescence measured in 50 experiments over a 10-min period), corresponding to anion concentrations of 85 μM iodide and 50 μM perchlorate.

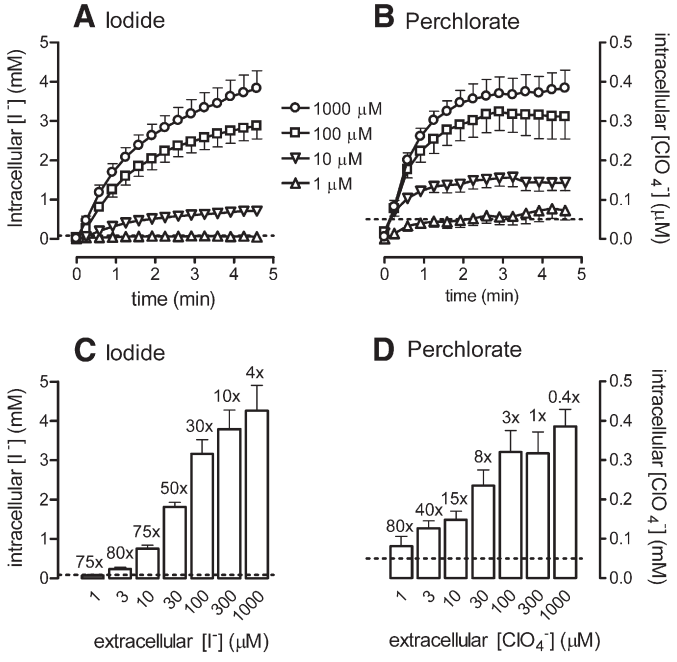

Fig. 4. Quantitation of perchlorate and iodide uptake in FRTL-5 cells. Cells were exposed to anions (1–1000 μM) for 5 min, and fluorescence changes were converted into intracellular concentrations using the affinity of purified YFP-H148Q/I152L determined in FRTL-5 cells *in situ*. Panels A and B show the time courses of iodide and perchlorate uptake respectively, in response 1 μM (△), 10 μM (▽), 100 μM (□) and 1000 μM (○) extracellular anions. Panels C and D show the steady-state intracellular concentration of iodide and perchlorate respectively. Numbers above bars represent the intracellular-to-extracellular concentration ratio. Dotted lines represent the limit of detection of intracellular iodide (85 μM) and perchlorate (50 μM). Points and bars represent mean ± SE of 6 experiments.

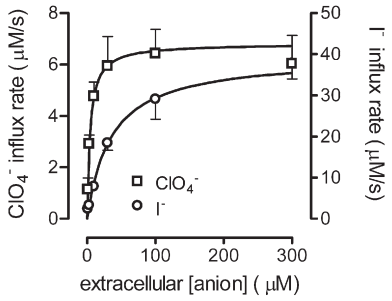

Fig. 5. Michaelis–Menten plot of perchlorate and iodide uptake, showing the maximal rate of iodide (○) and perchlorate (□) influx as a function of extracellular anion concentration. Points represent mean ± SE of 6 experiments.

Exposure of FRTL-5 cells to extracellular iodide or perchlorate (1–1000 μM) resulted in a time- and concentration-dependent increase in the intracellular concentration to levels at or above the detection limit for each ion (Fig. 4). Intracellular concentration increased with time according to a one-phase exponential association function. Perchlorate accumulation was more rapid than iodide accumulation, with half-times of 0.59 ± 0.10 min for perchlorate and 1.18 ± 0.11 min for iodide, independent of extracellular concentration ($p<0.0001$ *t*-test, $n=6$ at each extracellular concentration). Steady-state intracellular-to-extracellular concentration ratios were up to 75–80× for both anions, and decreased with increasing extracellular anion concentrations. At all extracellular concentrations >1 μM, intracellular-to-extracellular concentration ratios were greater for iodide than for perchlorate, suggesting that thyroid cells are more efficient at concentrating iodide than perchlorate. Indeed, intracellular iodide reached the millimolar concentration range, whereas intracellular perchlorate did not exceed 500 μM. Perchlorate and iodide uptake obeyed Michealis–Menten kinetics (Fig. 5), with perchlorate uptake characterized by a higher affinity (K_m 4.6 μM for perchlorate and 34.8 μM for iodide) and lower maximal velocity (V_{max} 6.8 μM/s for perchlorate and 39.5 μM/s for iodide).

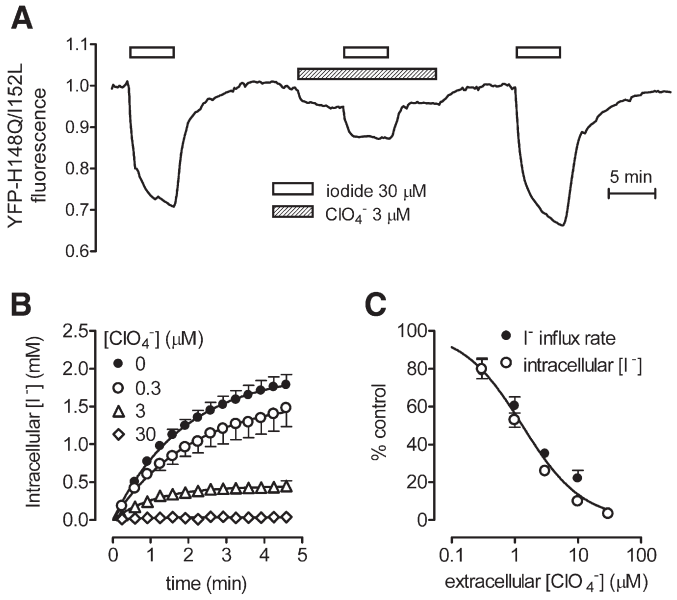

Fig. 6. Inhibition of NIS-mediated iodide uptake in FRTL-5 cells by perchlorate. (A) Representative tracing demonstrating changes in YFP-H148Q/I152L fluorescence induced by iodide in the absence and presence of perchlorate. (B) Time course of iodide accumulation induced by 30 μM extracellular iodide in the presence of 0 (●), 0.3 μM (○), 3 μM (△) and 30 μM (◊) extracellular perchlorate. (C) Perchlorate-induced inhibition of the initial rate of iodide uptake (●) and steady-state intracellular concentration (○). Points represent mean ± SE of 6–7 experiments.

Inhibition of iodide uptake in FRTL-5 thyroid cells by perchlorate

NIS inhibition by perchlorate was assessed as the ability of perchlorate to prevent iodide-induced changes in YFP-H148Q/I152L fluorescence in FRTL-5 cells (Fig. 6). Pre-treatment of cells for 5 min with 0.3–30 μM perchlorate caused a concentration-dependent inhibition of iodide uptake, both in terms of the initial rate of influx (IC_{50} 1.6 μM; log IC_{50} -5.80 ± 0.05, $n=6$ at each perchlorate concentration) and steady-state intracellular concentration (IC_{50} 1.1 μM; log IC_{50} -5.95 ± 0.03, $n=6$ at each perchlorate concentration). Inhibition of iodide uptake was complete at 30 μM perchlorate, and was fully reversible following rinsing with PBS.

Effect of perchlorate on YFP-H148Q/I152L fluorescence in hNIS-expressing COS-7 cells

In order to confirm that NIS transports perchlorate, the effect of perchlorate on YFP-H148Q/I152L fluorescence was examined in COS-7 cells expressing NIS following co-transfection with hNIS and YFP-H148Q/I152L cDNAs (Fig. 7). NIS functionality was confirmed as iodide-induced suppression of cellular YFP-H148Q/I152L fluorescence. Both perchlorate and iodide (1–1000 μM) induced concentration-dependent decreases in YFP-H148Q/I152L fluorescence in COS-7 cells expressing hNIS, but had no effect (<2%) in COS-7 cells lacking hNIS (Fig. 6). Perchlorate induced a significantly smaller decrease in fluorescence ($10.6 \pm 1.1\%$ at 1 mM, $n=5$) than iodide ($31.8 + 3.1\%$ at 1 mM iodide, $n=6$) ($p<0.001$, unpaired *t*-test).

Discussion

The present study describes an innovative approach to detect cellular uptake of the environmental contaminant perchlorate based upon live-cell imaging with YFP-H148Q/I152L as a genetically-encodable fluorescent biosensor. In recent years, fluorescent sensors have been increasingly used to detect endogenous and exogenous substances in biological samples, including living cells. Fluorescent sensors provide a simple technique to measure analyte concentrations without the need for highly-sophisticated instrumentation, and are particularly suited to the dynamic internal milieu of cells. Synthetic chemosensors have been used to monitor the cellular uptake of several pollutant ions, primarily toxic heavy metal ions such as Hg^{2+}, Cd^{2+} and Pb^{+} and Cr^{3+} (He et al., 2006; Taki et al., 2008; Zhou et al., 2008; Huang et al., 2009). Genetically-encoded fluorescent proteins been extensively used to detect ions and molecules normally present within cells, but their application to the detection of environmental contaminants is limited. Recently, a mercury-sensitive GFP variant was used as a biosensor of mercury(II) uptake by bacterial cells and *Caenorhabditis elegans* (Chapleau et al., 2008 and Chapleau and Sagermann, 2009). The current demonstration that YFP-H148Q/I152L can act as an intracellular perchlorate biosensor represents a significant advancement in the development of tools to monitor the accumulation of pollutant ions by mammalian cells.

YFP-H148Q/I152L, like its parent protein YFP, is a barrel-shaped protein with a tri-peptide chromophore buried within its cylinder (Elsliger et al., 1999; Wachter and Remington, 1999; Galietta et al., 2001a, 2001b). Previous studies have shown that YFP-H148Q/I152L fluorescence is suppressed by monovalent anions with an order of potency of $I^- > F^- > NO_3^- > Br^- > Cl^-$ (Galietta et al., 2001a). Anions bind to a unique binding site close to but distinct from the tripeptide chromophore, and suppress fluorescence as a result of chromophore protonation (Jayaraman et al., 2000; Wachter et al., 2000). The halide-sensitivity of YFPs has been used to measure intracellular chloride and iodide concentrations in mammalian cells, and to monitor halide transport across the cell membrane via anion channels and transporters (Galietta et al. 2001b; Rhoden et al., 2007; Markova et al., 2008). In the present study, we demonstrate that YFP-H148Q/I152L fluorescence is suppressed by perchlorate with a high affinity (~1 mM) equal to that of iodide. Another YFP variant, YFP-H148Q, has a lower affinity (21 mM) for both perchlorate and iodide (Jayaraman et al., 2000), suggesting that the I152L substitution is critical in determining sensitivity to these two anions.

Expressing YFP-H148Q/I152L in thyroid cells has enabled the direct detection of intracellular perchlorate, not previously possible with other techniques. Indeed, the ability of NIS to transport perchlorate has been the subject of much debate due to the difficulty of measuring the anion in living systems (Wolff, 2002; Dohan et al.,

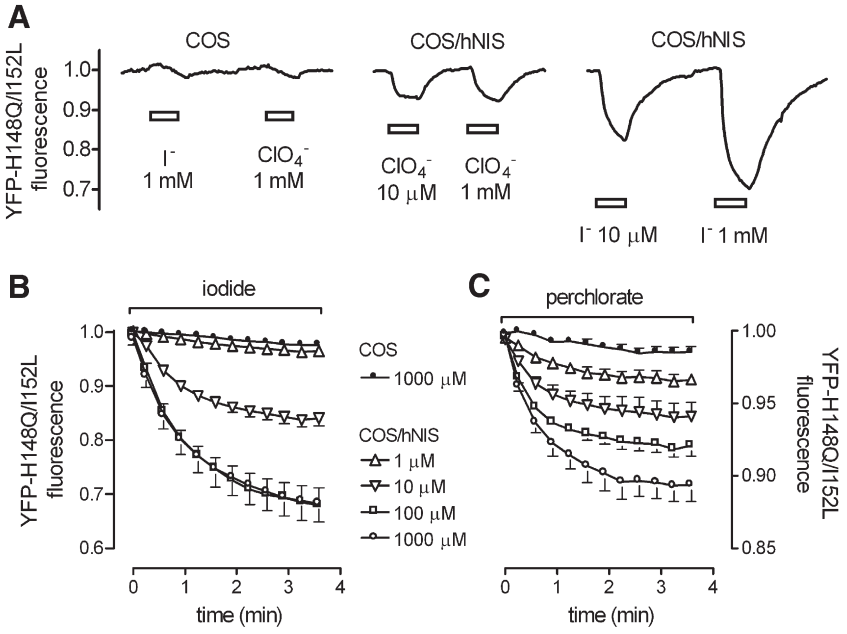

Fig. 7. Effect of perchlorate and iodide on YFP-H148Q/I152L fluorescence in NIS-expressing COS-7 cells. (A) Representative tracings illustrating iodide- and perchlorate-induced changes in fluorescence, normalized against resting fluorescence, in wild-type COS-7 cells (COS) and COS-7 cells transiently expressing human NIS (COS/hNIS). Panels (B) and (C) show the time course of fluorescence changes induced by extracellular iodide and perchlorate respectively, in COS/hNIS cells exposed to 1 μM (△), 10 μM (▽), 100 μM (□) and 1000 μM (○) anions, and COS cells exposed to 1000 μM (●) anions. Data points represent mean ± SE of 4–6 experiments.

2003; Clewell et al., 2004). Several studies demonstrated $^{36}ClO_4^-$ accumulation by the thyroid gland *in vivo* in rats and man (Anbar et al., 1959; Chow et al., 1969; Chow and Woodbury, 1970; Yu et al., 2002), however, possible contamination with other ^{36}Cl species including $^{36}ClO_3^-$, have raised questions as to the identity of the transported radioisotope in early studies. *In vitro* radiotracer uptake assays to measure NIS-mediated perchlorate transport are not possible due to the low specific activity of $^{36}ClO_4^-$. Electrophysiological studies revealed steady-state inward electrical currents in NIS-expressing cells in response to iodide but not perchlorate (Eskandari et al., 1997; Yoshida et al., 1997, 1998). Indirect functional evidence for perchlorate transport by NIS was recently provided in a bicameral model of vectorial transport using polarized kidney epithelial cells expressing a partial NIS protein targeted to the apical membrane (Dohan et al., 2007). In this system, $^{125}I^-$ was transported from the apical chamber to the basolateral chamber, and this transport was delayed by apical perchlorate. The delay in $^{125}I^-$ transport implies a gradual decrease in the concentration of apical perchlorate due to its own translocation to the basolateral chamber, ultimately lifting the inhibitory effect of perchlorate on iodide fluxes. Furthermore, translocated perchlorate collected from the basolateral chamber was able to inhibit $^{125}I^-$ uptake by non-polarized cells expressing wild-type NIS. Direct chemical detection of perchlorate in thyroid cells was recently achieved using ion chromatography-electrospray ionization-tandem mass spectrometry (Tran et al., 2008). FRTL-5 thyroid cells were equilibrated in a perchlorate-containing medium, and after a rapid rinse, total perchlorate content was measured in the cell lysate (Tran et al., 2008). Perchlorate accumulation was competitively inhibited by iodide and increased by TSH, consistent with NIS-mediated transport. In contrast to chemical methods, detection of perchlorate with YFP-H148Q/I152L permits the free cytoplasmic concentration to be monitored in real time allowing the kinetics of influx by NIS to be readily studied.

The sensitivity of YFP-H148Q/I152L to iodide as well as perchlorate was used to compare the cellular uptake of the two anions. Iodide was accumulated by FRTL-5 cells to higher intracellular concentrations than perchlorate. The accuracy of perchlorate quantification can be questioned given that perchlorate induces, at most, a 10–12% decrease in cellular fluorescence in intact cells, and the sensitivity of YFP-H148Q/I152L is not optimal for measurement of sub-millimolar perchlorate concentrations. Nevertheless, the similar affinity of YFP-H148Q/I152L for iodide and perchlorate suggests that the smaller effect of perchlorate on cellular fluorescence reflects true differences in the intracellular accumulation of the two anions.

Perchlorate uptake by FRTL-5 cells exhibited a higher affinity and lower V_{max} compared with iodide uptake. Iodide uptake by NIS-expressing cells has been extensively studied with radiotracers and electrophysiological techniques, and is characterized by an affinity of 30–35 μM similar to that obtained with YFP-H148Q/I152L (Weiss et al., 1984; Dai et al., 1996; Kosugi et al., 1996; Smanik et al., 1996). The kinetics of perchlorate transport, in contrast, have not been measured. Perchlorate is known to inhibit NIS with a potency of 1–2 μM, based upon inhibition of radioiodide uptake and iodide-induced currents in NIS expressing cells (Eskandari et al., 1997; Van Sande et al., 2003; Tonacchera et al. 2004). Using YFP-H148Q/I152L, a similar inhibitory constant of 1 μM was obtained. Perchlorate uptake exhibited a slightly lower affinity (4.6 μM), probably reflecting intracellular perchlorate concentrations that are close to the limit of detection of YFP-H148Q/I152L. The inhibitory constant, in contrast, is independent of the sensitivity of YFP-H148Q/I152L for perchlorate, reflecting from the ability of perchlorate to prevent iodide-induced changes in YFP-H148Q/I152L fluorescence. The lower V_{max} of perchlorate uptake compared with iodide uptake likely accounts for the lower intracellular concentration at equilibrium. A physiologically based pharmacokinetic model of perchlorate and iodide distribution in the male rat incorporates affinity constants for thyroidal NIS of 31.5 μM iodide and 1.8 μM perchlorate, and predicts a V_{max} for transport into the thyroid follicle approximately one order of magnitude lower for perchlorate than for iodide (Merrill et al., 2003). The kinetic parameters identified in this study may help refine pharmacokinetic models of perchlorate distribution in the body for the assessment of the health effects of this pollutant.

The kinetics of perchlorate uptake identified in this study are similar to those of perrhenate, which is also transported by NIS with a higher affinity and lower V_{max} than iodide (Zuckier et al., 2004; Dohan et al., 2007). The reduced V_{max} of perrhenate versus iodide uptake is thought to reflect the different stoichiometries of Na^+/anion transport, 2:1 for iodide and 1:1 for perrhenate. Perrhenate uptake can be measured with $^{186}ReO_4^-$ and shows a hyperbolic dependence on extracellular Na^+ concentration. Perchlorate uptake by FRTL-5 cells in this study was Na^+-dependent, however, the stoichiometry of transport could not be determined due the small size of perchlorate-induced changes in cellular YFP-H148Q/I152L fluorescence.

Health concerns over perchlorate exposure centre on inhibition of thyroidal iodide uptake as its only mode of action (NRC, 2005). What then are the consequences of perchlorate transport by NIS? Perchlorate is unreactive, and is not metabolized in the body with over 99% of an administered dose appearing in urine unchanged (Anbar et al., 1959; Yu et al., 2002). Perchlorate sequestered by the thyroid gland is concentrated in the follicular lumen, but unlike iodide, is not organified and is released back into the bloodstream. Perchlorate-induced changes in YFP-H148Q/I152L fluorescence in FRTL-5 cells are fully and rapidly reversed within minutes, suggesting that perchlorate is not compartmentalized within cells or bound to intracellular proteins (or at levels below the sensitivity of the method). In contrast, perchlorate clearance from the thyroid gland *in vivo* takes place over several hours, possibly reflecting the slower release of perchlorate from the thyroid lumen (Yu et al., 2002). Recent pharmacokinetic studies in rats suggest that inhibition of thyroidal iodide uptake does not adequately describe perturbations in serum thyroxine and TSH levels, and the authors propose that additional mechanisms may be involved such as inhibition of thyroid hormone synthesis or secretion (McLanahan et al., 2009). High concentrations of perchlorate (>100 μM) have been found to inhibit incorporation of iodide into iodotyrosines in the isolated thyroid gland (Greer et al., 1966). In contrast, other studies have found no effect of perchlorate (>100 μM) on iodide organification or thyroid peroxidase activity (Alexander, 1959; Magnusson et al; 1984). Clearly, further studies are needed to identify potential sites of interaction of thyroidal perchlorate.

NIS-mediated transport of perchlorate is more likely to have health-related effects in other NIS-expressing tissues, such as the breast and placenta. NIS expression is induced in the mammary gland during lactation and mediates iodide transport into milk, supplying the nursing infant with dietary iodide (Tazebay et al., 2000). Perchlorate has been detected in human and dairy milk (Kirk et al., 2005; Pearce et al., 2007), and milk samples from lactating rats injected with perchlorate inhibit radioiodide uptake *in vitro* (Dohan et al., 2007). NIS is also present in the placenta where it mediates the transfer of iodide to the fetus (Bidart et al., 2000; Mitchell et al., 2001). Perchlorate crosses the placental barrier in guinea pigs (Postel, 1957) and has been detected in human amniotic fluid samples (Blount and Valentine-Blasini, 2006). Given the critical role of thyroid hormones in growth and development, there is a particular concern over the potential consequences of perchlorate exposure in fetuses and newborns. Application of the YFP-based assay to mammary epithelial cells and trophoblasts may be particularly useful to measure the capacity of these cell types to accumulate perchlorate. In principle, the YFP-based assay can be applied to any NIS-expressing cell type in culture, so long as cells can be induced to express YFP-H148Q/I152L using standard gene transfer methodologies. The commercial availability of a modified baculovirus (Bacmam) vector containing the YFP-H148Q/I152L gene (Premo Halide Sensor, Invitrogen Inc.) may allow

the biosensor to be used in difficult-to-transfect cell types, such as human primary cell cultures.

The present study describes an innovative approach to detect the cellular uptake of perchlorate and characterize the kinetics of transport by NIS. Uptake was monitored in the presence of 1–1000 μM extracellular perchlorate, reflecting the concentration range producing measurable alterations in cellular YFP-H148Q/I152L fluorescence. Environmental exposure to perchlorate, however, is likely to result in serum perchlorate levels less than 1 μM. Research aimed at developing biosensors with improved perchlorate-sensitivity, for example through mutagenesis of YFP-H148Q/I152L at positions close to the anion binding site, may provide tools to measure the cellular uptake of environmental perchlorate and evaluate its biological implications. The development of biosensors that are sensitive to other pollutants may represent a new strategy to monitor their cellular accumulation and facilitate the evaluation of their toxic and other health-related effects.

Conflict of interest statement
The authors declare that there are no conflicts of interest.

Acknowledgments

This work was funded by *Programma Incentivazione alla Mobilità di Studiosi Stranieri e Italiani Residenti all' Estero "Rientro dei Cervelli"* and PRIN 2006 awards from the Ministero dell'Istruzione, dell'Università e della Ricerca of Italy (K.J.R.), a Doctoral Fellowship from the Fondazione Carisbo (S.C.) and a Post-Doctoral Fellowship from the University of Bologna (J.D.B.).

References

Alexander, N.M., 1959. Iodide peroxidase in rat thyroid and salivary glands and its inhibition by antithyroid compounds. J. Biol. Chem. 234, 1530–1533.
Ambesi-Impiombato, F.S., Parks, L.A., Coon, H.G., 1980. Culture of hormone-dependent functional epithelial cells from rat thyroids. Proc. Natl. Acad. Sci. U.S.A. 77, 3455–3459.
Anbar, M., Guttmann, S., Lewitus, Z., 1959. The mode of action of perchlorate ions on the iodine uptake of the thyroid gland. Int. J. Appl. Radiat. Isot. 7, 87–96.
Bidart, J.M., Lacroix, L., Evain-Brion, D., Caillou, B., Lazar, V., Frydman, R., Bellet, D., Filetti, S., Schlumberger, M., 2000. Expression of Na+/I- symporter and Pendred syndrome genes in trophoblast cells. J. Clin. Endocrinol. Metab. 85, 4367–4372.
Blount, B.C., Valentin-Blasini, L., 2006. Analysis of perchlorate, thiocyanate, nitrate and iodide in human amniotic fluid using ion chromatography and electrospray tandem mass spectrometry. Anal. Chim. Acta 567, 87–93.
Chapleau, R.R., Sagermann, M., 2009. Real-time *in vivo* imaging of mercury uptake in Caenorhabditis elegans through the foodchain. Toxicology 261, 136–142.
Chapleau, R.R., Blomberg, R., Ford, P.C., Sagermann, M., 2008. Design of a highly specific and noninvasive biosensor suitable for real-time *in vivo* imaging of mercury (II) uptake. Protein Sci. 17, 614–622.
Chow, S.Y., Woodbury, D.M., 1970. Kinetics of distribution of radioactive perchlorate in rat and guinea-pig thyroid glands. J. Endocrinol. 47, 207–218.
Chow, S.Y., Chang, L.R., Yen, M.S., 1969. A comparison between the uptakes of radioactive perchlorate and iodide by rat and guinea-pig thyroid glands. J. Endocrinol. 45, 1–8.
Clewell, R.A., Merrill, E.A., Narayanan, L., Gearhart, J.M., Robinson, P.J., 2004. Evidence for competitive inhibition of iodide uptake by perchlorate and translocation of perchlorate into the thyroid. Int. J. Toxicol. 23, 17–23.
Dai, G., Levy, O., Carrasco, N., 1996. Cloning and characterization of the thyroid iodide transporter. Nature 379, 458–460.
Dohan, O., De la Vieja, A., Paroder, V., Riedel, C., Artani, M., Reed, M., Ginter, C.S., Carrasco, N., 2003. The sodium/iodide symporter (NIS): characterization, regulation, and medical significance. Endocr. Rev. 24, 48–77.
Dohán, O., Portulano, C., Basquin, C., Reyna-Neyra, A., Amzel, L.M., Carrasco, N., 2007. The Na+/I- symporter (NIS) mediates electroneutral active transport of the environmental pollutant perchlorate. Proc. Natl. Acad. Sci. U.S.A. 104, 20250–20255.
Elsliger, M.A., Wachter, R.M., Hanson, G.T., Kallio, K., Remington, S.J., 1999. Structural and spectral response of green fluorescent protein variants to changes in pH. Biochemistry 38, 5296–5301.
Eskandari, S., Loo, D.D., Dai, G., Levy, O., Wright, E.M., Carrasco, N., 1997. Thyroid Na^+/I^- symporter. Mechanism, stoichiometry, and specificity. J. Biol. Chem. 272, 27230–27238.
Galietta, L.J., Haggie, P.M., Verkman, A.S., 2001a. Green fluorescent protein-based halide indicators with improved chloride and iodide affinities. FEBS Lett. 499, 220–224.
Galietta, L.V., Jayaraman, S., Verkman, A.S., 2001b. Cell-based assay for high-throughput quantitative screening of CFTR chloride transport agonists. Am. J. Physiol. 281, C1734–C1742.
Greer, M.A., Stott, A.K., Milne, K.A., 1966. Effects of thiocyanate, perchlorate and other anions on thyroidal iodine metabolism. Endocrinology 79, 237–247.
He, Q., Miller, E.W., Wong, A.P., Chang, C.J., 2006. A selective fluorescent sensor for detecting lead in living cells. J. Am. Chem. Soc. 128, 9316–9317.
Huang, W., Zhou, P., Yan, W., He, C., Xiong, L., Li, F., Duan, C., 2009. A bright water-compatible sugar-rhodamine fluorescence sensor for selective detection of Hg^{2+} in natural water and living cells. J. Environ. Monit. 11, 330–335.
Interstate Technology & Regulatory Council (ITRC) Perchlorate Team, 2005. Perchlorate: Overview of Issues, Status, and Remedial Options. ITRC, Washington DC.
Jackson, W.A., Joseph, P., Laxman, P., Tan, K., Smith, P.N., Yu, L., Anderson, T.A., 2005. Perchlorate accumulation in forage and edible vegetation. J. Agric. Food Chem. 53, 369–373.
Jayaraman, S., Haggie, P., Wachter, R.M., Remington, S.J., Verkman, A.S., 2000. Mechanism and cellular applications of a green fluorescent protein-based halide sensor. J. Biol. Chem. 275, 6047–6050.
Kirk, A.B., Smith, E.E., Tian, K., Anderson, T.A., Dasgupta, P.K., 2003. Perchlorate in milk. Env. Sci. Technol. 37, 4979–4981.
Kirk, A.B., Martinelango, P.K., Tian, K., Dutta, A., Smith, E.E., Dasgupta, P.K., 2005. Perchlorate and iodide in dairy and breast milk. Environ. Sci. Technol. 39, 2011–2017.
Kosugi, S., Sasaki, N., Hai, N., Sugawa, H., Aoki, N., Shigemasa, C., Mori, T., Yoshida, A., 1996. Establishment and characterization of a Chinese hamster ovary cell line, CHO-4J, stably expressing a number of Na+/I- symporters. Biochem. Biophys. Res. Commun. 227, 94–101.
Magnusson, R.P., Taurog, A., Dorris, M.L., 1984. Mechanisms of thyroid peroxidase- and lactoperoxidase-catalyzed reactions involving iodide. J. Biol. Chem. 259, 13783–13790.
Markova, O., Mukhtarov, M., Real, E., Jacob, Y., Bregestovski, P., 2008. Genetically encoded chloride indicator with improved sensitivity. J. Neurosci. Methods 170, 67–76.
McLanahan, E.D., Andersen, M.E., Campbell, J.L., Fisher, J.W., 2009. Competitive inhibition of thyroidal uptake of dietary iodide by perchlorate does not describe perturbations in rat serum total T4 and TSH. Environ. Health Perspect. 117, 731–738.
Merrill, E.A., Clewell, R.A., Gearhart, J.M., Robinson, P.J., Sterner, T.R., Yu, K.O., Mattie, D.R., Fisher, J.W., 2003. PBPK predictions of perchlorate distribution and its effect on thyroid uptake of radioiodide in the male rat. Toxicol. Sci. 2003 (73), 256–269.
Mitchell, A.M., Manley, S.W., Morris, J.C., Powell, K.A., Bergert, E.R., Mortimer, R.H., 2001. Sodium iodide symporter (NIS) gene expression in human placenta. Placenta 22, 256–258.
Murray, C.W., Egan, S.K., Kim, H., Beru, N., Bolger, P.M., 2008. US Food and Drug Administration's Total Diet Study: dietary intake of perchlorate and iodine. J. Expo. Sci. Environ. Epidemiol. 18, 571–580.
National Research Council, 2005. Health Implications of Perchlorate Ingestion. National Academies Press, Washington DC.
Pearce, E.N., Leung, A.M., Blount, B.C., Bazrafshan, H.R., He, X., Pino, S., Valentin-Blasini, L., Braverman, L.E., 2007. Breast milk iodine and perchlorate concentrations in lactating Boston-area women. J. Clin. Endocrinol. Metab. 92, 1673–1677.
Postel, S., 1957. Placental transfer of perchlorate and triiodothyronine in the guinea pig. Endocrinology 60, 53–66.
Rhoden, K.J., Cianchetta, S., Stivani, V., Portulano, C., Galietta, L.J.V., Romeo, G., 2007. Cell-based imaging of sodium iodide symporter activity with the yellow fluorescent protein variant YFP-H148Q/I152L. Am. J. Physiol. 292, C814–C823.
Rhoden, K.J., Cianchetta, S., Duchi, S., Romeo, G., 2008. Fluorescence quantitation of thyrocyte iodide accumulation with the yellow fluorescent protein variant YFP-H148Q/I152L. Anal. Biochem. 373, 239–246.
Sanchez, C.A., Crump, K.S., Krieger, R.I., Khandaker, N.R., Gibbs, J.P., 2005. Perchlorate and nitrate in leafy vegetables of North America. Environ. Sci. Technol. 39, 9391–9397.
Smanik, P.A., Liu, Q., Furminger, T.L., Ryu, K., Xing, S., Mazzaferri, E.L., Jhiang, S.M., 1996. Cloning of the human sodium lodide symporter. Biochem. Biophys. Res. Commun. 226, 339–345.
Srinivasan, A, Viraraghavan, T., 2009. Perchlorate: health effects and technologies for its removal from water resources. Int. J. Environ. Res. Public Health 6, 1418–1442.
Taki, M., Desaki, M., Ojida, A., Iyoshi, S., Hirayama, T., Hamachi, I., Yamamoto, Y., 2008. Fluorescence imaging of intracellular cadmium using a dual-excitation ratiometric chemosensor. J. Am. Chem. Soc. 130, 12564–12565.
Tazebay, U.H., Wapnir, I.L., Levy, O., Dohan, O., Zuckier, L.S., Zhao, Q.H., Deng, H.F., Amenta, P.S., Fineberg, S., Pestell, R.G., Carrasco, N., 2000. The mammary gland iodide transporter is expressed during lactation and in breast cancer. Nat. Med. 6, 871–878.
Thomas, J.A., Buchsbaum, R.N., Zimniak, A., Racker, E., 1979. Intracellular pH measurements in Ehrlich ascites tumor cells utilizing spectroscopic probes generated *in situ*. Biochemistry 18, 2210–2218.
Tonacchera, M., Pinchera, A., Dimida, A., Ferrarini, E., Agretti, P., Vitti, P., Santini, F., Crump, K., Gibbs, J., 2004. Relative potencies and additivity of perchlorate, thiocyanate, nitrate, and iodide on the inhibition of radioactive iodide uptake by the human sodium iodide Symporter. Thyroid 14, 1012–1019.
Tran, N., Valentín-Blasini, L., Blount, B.C., McCuistion, C.G., Fenton, M.S., Gin, E., Salem, A., Hershman, J.M., 2008. Thyroid-stimulating hormone increases active transport of perchlorate into thyroid cells. Am. J. Physiol. 294, E802–E806.
US E.P.A., 2008a. Drinking water: preliminary regulatory determination on perchlorate. EPA-HQ-OW-2008-0692. Federal Register 73, 60262–60282.
US E.P.A., 2008b. Interim Drinking Water Health Advisory for Perchlorate. EPA 822-R-08-25.

Van Sande, J., Massart, C., Beauwens, R., Schoutens, A., Costagliola, S., Dumont, J.E., Wolff, J., 2003. Anion selectivity by the sodium iodide symporter. Endocrinology 144, 247–252.

Wachter, R.M., Remington, S.J., 1999. Sensitivity of the yellow variant of green fluorescent protein to halides and nitrate. Curr. Biol. 9, R628–629.

Wachter, R.M., Yarbrough, D., Kallio, K., Remington, S.J., 2000. Crystallographic and energetic analysis of binding of selected anions to the yellow variants of green fluorescent protein. J. Mol. Biol. 301, 157–171.

Weiss, S.J., Philp, N.J., Grollman, E.F., 1984. Iodide transport in a continuous line of cultured cells from rat thyroid. Endocrinology 114, 1090–1098.

Wieth, J.O., Tosteson, M.T., 1979. Organotin-mediated exchange diffusion of anions in human red cells. J. Gen. Physiol. 73, 765–788.

Wolff, J., 2002. A miss for NIS? Thyroid 12, 295–297.

Wuthier, U., Pham, H.V., Zuend, R., Welti, D., Funck, R.J.J., Bezegh, A., Ammann, D., Pretsch, E., Simon, S., 1984. Tin organic compounds as neutral carriers for anion selective electrodes. Anal. Chem. 56, 535–538.

Yoshida, A., Sasaki, N., Mori, A., Taniguchi, S., Mitani, Y., Ueta, Y., Hattori, K., Sato, R., Hisatome, I., Mori, T., Shigemasa, C., Kosugi, S., 1997. Different electrophysiological character of I^-, ClO_4^-, and SCN^- in the transport by Na^+/I^- symporter. Biochem. Biophys. Res. Commun. 231, 731–734.

Yoshida, A., Sasaki, N., Mori, A., Taniguchi, S., Ueta, Y., Hattori, K., Tanaka, Y., Igawa, O., Tsuboi, M., Sugawa, H., Sato, R., Hisatome, I., Shigemasa, C., Grollman, E.F., Kosugi, S., 1998. Differences in the electrophysiological response to I^- and the inhibitory anions SCN^- and ClO_4^-, studied in FRTL-5 cells. Biochim. Biophys. Acta 1414, 231–237.

Yu, K.O., Narayanan, L., Mattie, D.R., Godfrey, R.J., Todd, P.N., Sterner, T.R., Mahle, D.A., Lumpkin, M.H., Fisher, J.W., 2002. The pharmacokinetics of perchlorate and its effect on the hypothalamus–pituitary–thyroid axis in the male rat. Toxicol. Appl. Pharmacol. 182, 148–159.

Zhou, Z., Yu, M., Yang, H., Huang, K., Li, F., Yi, T., Huang, C., 2008. FRET-based sensor for imaging chromium(III) in living cells. Chem. Commun. (Camb.) 29, 3387–3389.

Zuckier, L.S., Dohan, O., Li, Y., Chang, C.J., Carrasco, N., Dadachova, E., 2004. Kinetics of perrhenate uptake and comparative biodistribution of perrhenate, pertechnetate, and iodide by NaI symporter-expressing tissues *in vivo*. J. Nucl. Med. 45, 500–507.